IOP Conf. Series: Materials Science and Engineering **116** (2016) 012004 doi:10.1088/1757-899X/116/1/012004

Surface modification of additive manufactured Ti6Al4V alloy with Ag nanoparticles: wettability and surface morphology study

E Chudinova[1], M Surmeneva[1], A Koptioug[2], A Sharonova[1], K Loza[3] and R Surmenev[1]

[1] Tomsk Polytechnic University, Institute of Physics and Technologies, 30, Lenina ave., Tomsk 634050, Russia
[2] Mid Sweden University, Akademigatan 1, Östersund SE-831 25 , Sweden
[3] Inorganic Chemistry and Center for Nanointegration Duisburg-Essen (CeNIDE), University of Duisburg-Essen, Essen 45117, Germany

E-mail: rsurmenev@mail.ru

Abstract. In this work, the use of electrophoretic deposition to modify the surface of Ti6Al4V alloy fabricated via additive manufacturing technology is reported. Poly(vinylpyrrolidone) (PVP)-stabilized silver nanoparticles (AgNPs) had a spherical shape with a diameter of the metallic core of 100±20 nm and ζ -potential -15 mV. The AgNPs- coated Ti6Al4V alloy was studied in respect with its chemical composition and surface morphology, water contact angle, hysteresis, and surface free energy. The results of SEM microphotography analysis showed that the AgNPs were homogeneously distributed over the surface. Hysteresis and water contact angle measurements revealed the effect of the deposited AgNPs layer, namely an increased water contact angle and decreased contact angle hysteresis. However, the average water contact angle was 125° for PVP-stabilized-AgNPs-coated surface, whereas ethylene glycol gave the average contact angle of 17°. A higher surface energy is observed for AgNPs-coated Ti6Al4V surface (70.17 mN/m) compared with the uncoated surface (49.07 mN/m).

1. Introduction

Titanium alloy foams have significant application potential due to their light weight and exceptional, isotropic mechanical properties as well as high corrosion resistance [1]. These include multiple structural applications in aerospace, aeronautics and automotive systems which take advantage of density-compensated strength and stiffness at elevated temperatures [1]. Murr et al. [2] have also recently demonstrated that Ti6Al4V cellular foams produced by additive manufacturing (AM) using electron beam melting (EBM®) technology have innovative applications in the “next generation biomedical implants”.

The AM allows to create customized implants individual for the patients and clinical cases[3]. These applications are utilizing strongest advantages of the AM technologies such as freedom of component shapes, possibilities of computer optimization of the manufactured-to-be component functionality and properties, and good value for money in manufacturing one-off or small series of products [4]. These benefits are already recognized by medical implant manufacturers and practical surgeons[5]. There are certain medical applications, such as acetabular cups mass-produced in

Ti6Al4V by EBM®, which have been successfully implemented for years [6, 7]. There is also a wide variety of biomedical implants manufactured by EBM® technology that are under investigation, as for example, customized hip and knee implants or bone grafting, including craniofacial and maxillofacial replacements [2, 6, 8].

Electrophoretic deposition can be used to fabricate well-distributed particles layers on metallic surfaces [12]. The aim of this study is to generate the silver nanoparticles assembly on the as-manufactured Ti64 surfaces via electrophoretic deposition and investigate the wettability and surface free energy of the developed surface.

2. Materials and methods

2.1. Samples preparation

All the samples used were fabricated using Ti6Al4V ELI powder in ARCAM A2 EBM® machine (Arcam AB, Mölndal, Sweden) [13]. The Arcam machine also makes it possible to produce implants with designed porosity and cellular lattice surface structures that stimulate the osteointegration in the single process procedure[7]. All samples were coin-like discs 10 and 30 mm in diameter with flat surfaces. These discs were manufactured in a single batch with their surfaces normal to the melt layer h. The 3D-scaffolds were made in two different batches with identical parameter settings and same diamond-shaped basic lattice cells. All samples were carefully blasted in the ARCAM powder recovery system using the same precursor powder. Electrochemical etching was carried out at 30° C in the ethanol and 2-propanol solution of the aluminum chloride and zinc chloride with the stabilized dc current density 0.2 A/cm^2[14].

2.2. Synthesis and deposition of silver nanoparticles

The surfaces of as-manufactured Ti6Al4V samples were modified by electrophoretic deposition of silver nanoparticles. Wet chemical synthesis and characterization of Poly(vinylpyrrolidone) (PVP)-stabilized silver nanoparticles were reported elsewhere [15]. Prior to electrophoretic deposition, the silver nanoparticles were dispersed in ethanol. Electrophoretic deposition was carried out at a constant voltage of 50 V for 30 min. The distance between the two electrodes was maintained at 3 mm. The concentration of AgNPs in the dispersion was 60 mg L-1. PVP-stabilized silver nanoparticles had a spherical shape with a diameter of the metallic core of 100±20 nm and ζ -potential of -15 mV.

2.3. Characterization

The morphology and composition of the surfaces were determined using an ESEM Quanta 400 FEG scanning electron microscope (SEM), equipped with energy-dispersive X-ray spectroscopy unit (EDX; Genesis 4000, SUTW-Si(Li) detector) operating in a high vacuum.

Contact angle analysis was performed with an optical contact angle apparatus (OCA 15 Plus Data Physics Instruments GmbH, Germany), using the SCA20 software (Data Physics Instruments GmbH, Germany). The contact angle of water in air was measured by the sessile drop method. A minimum of 10 droplets (2 μL, 5 μL·s-1) of water, 3 droplets of diiodomethane or ethylene glycol were examined for each sample, and the resulting mean values of the contact angles were used for the calculations. The surface free energy was calculated using Owens-Wendt-Rabel-Kaelble (ORWK) method. Three different media (water, diiodomethane and ethylene glycol) were used for these calculations.

3. Results and discussion

Figure 1 illustrates the morphology of the as-manufactured Ti6Al4V alloy samples. Because powder-bed process is used for manufacturing, component surfaces have certain amount of partially-connected (fused) precursor powder grains (60-100 μm in diameter), which resulted in a relatively rough surface morphology. As clearly visible from the images metal surface contains a number of powder grains strongly and rather loosely attached to the bulk metal (Figure 1) providing a roughness with the spectrum ranging from nanometers to about 100 μm, a feature quite common for the powder bed AM

processes. It has been extensively reported that the microscale morphology significantly influences cell behavior such as adhesion, proliferation and differentiation in vitro and in vivo[16].

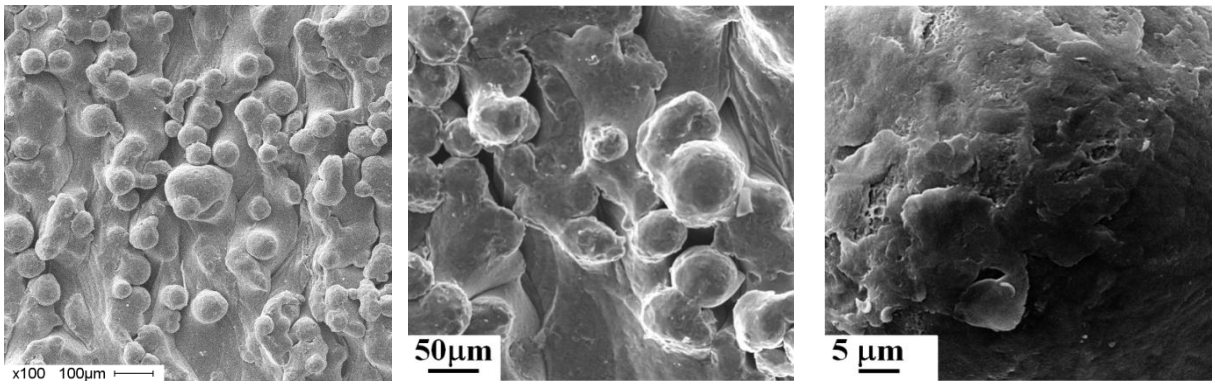

a b c

Figure 1. SEM images of the as-manufactured Ti6Al4V sample surface morphology. Samples are additively manufactured using EBM® technology . Images are acquired using SE detector.

Surfaces are also showing distinct roughness at the sub-micron scale (figure 1c).

According to the DLS measurement, the PVP-functionalized AgNPs were negatively charged ($\zeta = -15$ mV) particles with a hydrodynamic diameter of 100 ± 20 nm. The polydispersity index (PDI) was below 0.3, indicating the absence of large agglomerates.

SEM images of the AgNPson deposited on the surface of Ti6Al4V substrate are shown in Figure 2. A uniform distribution of the AgNPs was observed across the surface. The surface morphology of the initial Ti6Al4V substrate was not changed by the deposition of AgNPs. The metallic core diameter of the AgNPs determined from the SEM analysis was 110 ± 30 nm. The ordered AgNPs with well-defined two- (2D) and three-dimensional (3D) spatial configurations are expected to show the homogeneous and sustained release of Ag+ ions from nanoparticles to the surrounding tissue. These ions can reduce or even prevent colonization and subsequent biofilm formation on the surface of an implant. The further deposition of the hydroxiapatite (HA) film on the layer of AgNPs may improve this strategy since the release of silver ions from the AgNPs can be precisely controlled. It has already been shown that the use of HA film can help to control the Ag and Ni ions release [15, 17].

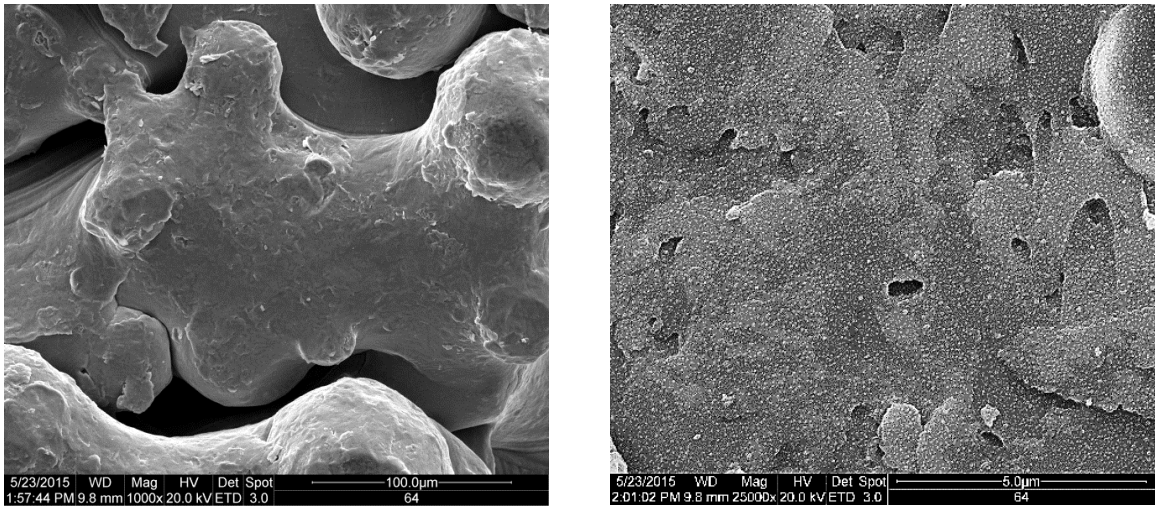

a b

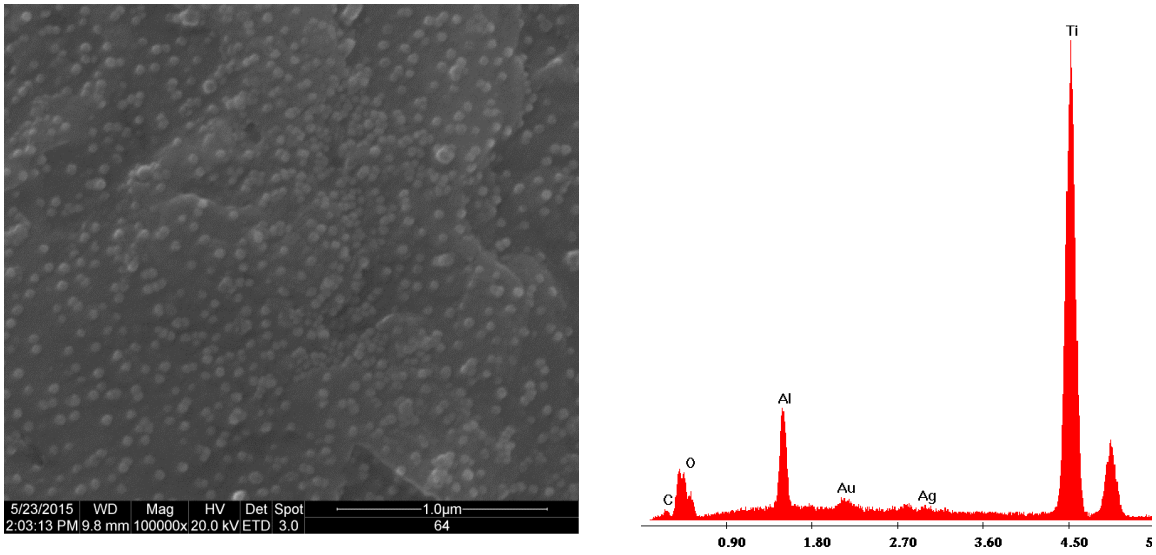

c d

Figure 2. SEM image (a-c) and EDX spectrum (d) of the Ti6Al4V alloy coated with AgNPs.

EDX spectrum analysis of the coated samples revealed that the obtained composite contained free silver. EDX analysis revealed silver concentrations of 0.58 at% for the silver nanoparticles deposited on the surface of Ti6Al4V alloy.

A detailed study of the wettability of the scaffold surfaces was done using contact angle sessile drop method and the contact angles for the scaffolds after modification with AgNPs before and after treatment are summarized in Table 1. It should be noted that water contact angle revealed the significant effect from the AgNPs layer. The hydrophobic and super-hydrophobic surfaces can result from the increased surface roughness, for example, this effect occurs naturally on the lotus leaf [18]. The surfaces of these leaves possess a micrometer-level roughness and they are covered with nanosized crystals of wax [18].

The highest contact angles were obtained with water, whereas ethylene glycol gave the lowest contact angles for PVP-stabilized-AgNPs-coated surface. One of the possible reasons for this effect may be due to the lower surface tension of ethylene glycol as compared to water, and as the consequence the AgNPs-coated samples can display a lower wetting resistance against ethyleneglycol [19]. Water (surface tension 72.8 mN m-1), diiodomethane (50.8 mN m-1) and ethylene glycol (48.0 mN m-1) were used as testing fluids. However, this must also be investigated in more details in the future[19]. The surface energy of materials is influenced by some surface characteristics like structure, morphology, roughness, chemical composition and surface charge, however, the correlation among them is not clear.

Figure 3 shows the variation of dispersive, polar and total surface energy of as-manufactured and modified surfaces of scaffolds. The results presented in Figure 3 show that total surface energy of the coated surfaces significantly varied from 29.22 to 70.17 mN/m compared with as-received Ti6Al4V scaffold (49.07 mN/m).

Sample	Contact angle, degrees			Contact angle hysteresis, degrees
	Water	Diiodmethan	Ethylene glycol	
Bare Ti6Al4V	106±1	34±1	42±2	20±3
HA-coated Ti6Al4V	109±2	56±2	80±1	16±1

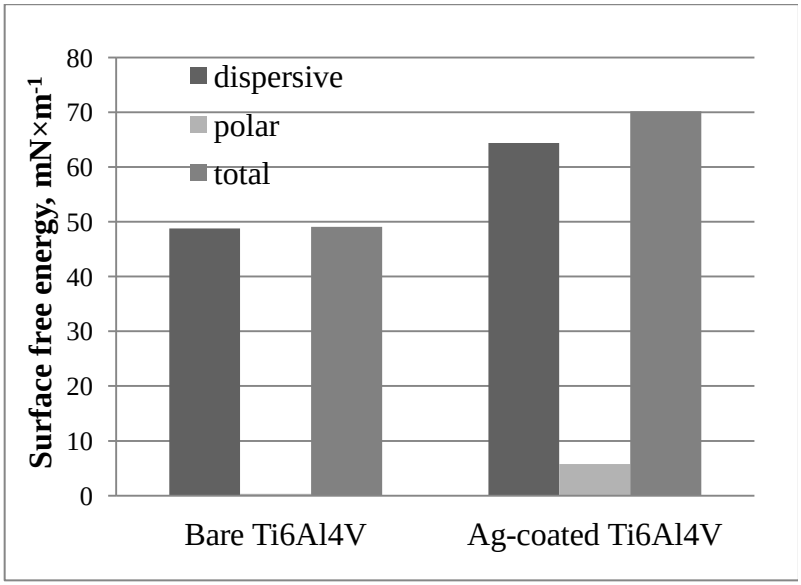

Figure 3. Variation of the dispersive, polar and total surface energy of as-manufactured and AgNPs-coated scaffolds surfaces.

A detailed comparison shows that a higher surface energy is observed for AgNPs-coated Ti6Al4V surface (70.17 mN/m) as compared to uncoated surface (49.07 mN/m). In nanoparticles, surfaces contribute to the chemical potential by creating surface free energy and surface stress [20]. Furthermore, the polar component of the surface energy is significantly higher for AgNPs-coated surface compared to the one of as-manufactured scaffolds. The dispersive component makes a major contribution of 0.1–8% to the total surface free energy for all the samples.

4. Conclusion

The Ti6Al4V alloy prepared via AM using EBM® technology was modified by electrophoretic deposition of AgNPs. The effect of the modification of the metallic scaffolds on the wettability and surface energy has been studied in details. The determined surface free energies of the AgNPs-coated Ti6Al4V scaffolds were significantly different from as-manufactured ones. A detailed comparison shows that a higher surface energy is observed for AgNPs-coated Ti6Al4V surfaces (70.17 mN/m) compared with uncoated ones (49.07 mN/m). The dispersive component made the major contribution to the total surface free energy for all the studied scaffolds. This resulted in the polar component making approximately a 0.1–8% contribution to the total surface free energy.

Acknowledgments

This research was supported by the *Russian Science Foundation* (15-13-00043).

References

[1] Murr L E, Gaytan S M, Medina F, Martinez E, Martinez J L, Hernandez D H, Machado B I, Ramirez D A, Wicker R B 2010 Characterization of Ti-6Al-4V open cellular foams fabricated by additive manufacturing using electron beam melting *Materials Science and Engineering* **527** 1861-1868.

[2] Murr L E, Gaytan S M, Medina F, Lopez H, Martinez E, Machado B I, Hernandez D H, Martinez L, Lopez M I, Wicker R B, Bracke J 2010 Next-generation biomedical implants using additive manufacturing of complex cellular and functional mesh arrays *Philos. Trans. R. Soc*. **368** 1999-2032.

[3] Koptyug A, Rännar L, Bäckström M, Fager Franzén S, Dérand P 2013 Additive manufacturing

technology applications targeting practical surgery *International Journal of Life Science and Medical Research* **3** 15-24.
[4] Cronskär M, Rännar L E, Bäckström M, Koptyug A 2008 Application of electron beam melting to titanium hip stem implants P*roc Intl Conference on Additive Technologies, Vienna, DAAAM International* 1559.
[5] Christensen A, Lippincott A, Kircher R 2007 An Introduction to Electron Beam Melting with Ti6Al4V-ELI for the Orthopaedic Device Industry *BONEZone* **6** 14-17.
[6] Herrera A, Yánez A, Martel O, Afonso H, Monopoli D 2014 Computational study and experimental validation of porous structures fabricated by electron beam melting: A challenge to avoid stress shielding *Materials Science and Engineering* C **45** 89-93.
[7] Thundal S 2008 Rapid manufacturing of orthopaedic implants *Adv. Mater. Process.* **166** 60-62.
[8] Cronskär M, Rännar L, Bäckström M 2013 Production of customized hip stem prostheses - a comparison between conventional machining and electron beam melting (EBM) *Rapid Prototyp. J.* **19** 365-372.
[9] Gristina A 1987 Biomaterial-centered infection: Microbial adhesion versus tissue integration. *Science* **237** 1588-1595.
[10] Lim P N, Chang L, Thian E S 2015 Development of nanosized silver-substituted apatite for biomedical applications: A review Nanomedicine: Nanotechnology, Biology, and Medicine, 2015. **11**: p. 1331–1344.
[11] Loza K, Diendorf J, Sengstock C, Ruiz-Gonzalez L, Gonzalez-Calbet J M, Vallet-Regi M, Köller M, Epple M 2014 The dissolution and biological effects of silver nanoparticles in biological media *J. Mater. Chem.* B **2** 1634-1643.
[12] Boccaccini A R, Keim S, Ma R, Li Y, Zhitomirsky I 2010 Electrophoretic deposition of biomaterials *J Royal Soc Interface* **7** S581-S613.
[13] Standard Specification for Additive Manufacturing Titanium-6 Aluminum-4 Vanadium ELI with Powder Bed Fusion; ASTM F2924–14; American Society for Testing Materials: West Conshohocken, P., USA, 2014.
[14] Tajima K, Hironaka M, Chen K K, Nagamatsu Y, Kakigawa H, Kozono Y 2008 Electropolishing of CP Titanium and Its Alloys in an Alcoholic Solution-based Electrolyte *Dent Mater J.* **27** 258-265.
[15] Ivanova A A, Surmenev R A, Surmeneva M A, Mukhametkaliyev T, Loza K, Prymak O, Epple M 2015 Hybrid biocomposite with a tunable antibacterial activity and bioactivity based on RF magnetron sputter deposited coating and silver nanoparticles *Applied Surface Science* **329** 212-218.
[16] Li L, Xie T 2005 Stem cell niche: structure and function *Annu. Rev. Cell Dev. Biol.* **21** 605-631.
[17] Surmenev R A, Ryabtseva M A, Shesterikov E V, Pichugin V F, Peitsch T, Epple M 2010 The release of nickel from nickel–titanium (NiTi) is strongly reduced by a sub-micrometer thin layer of calcium phosphate deposited by rf-magnetron sputtering *J. Mater. Sci.: Mater. Med*. **21**(4): p. 1233-1239.
[18] Wang C F, Chiou S F, Ko F H, Chou C T, Lin H C, Huang C F, Chang F C 2006 Fabrication of Biomimetic Super-Amphiphobic Surfaces Through Plasma Modification of Benzoxazine Films *Macromol. Rapid Commun.* **27** 333-337.
[19] Tang Z, Hess D W, V Breedveld V 2015 Fabrication of oleophobic paper with tunable hydrophilicity by treatment with non-fluorinated chemicals *J.Mater.Chem.* A **3** 14651 - 14660.
[20] Li W, Ni C, Lin H, Huang C P, S Ismat Shah 2004 Size dependence of thermal stability of TiO2 nanoparticles *Journal of Applied Physics* 96 6663-6668.